*Bulletin of the Geological Society of Malaysia, Volume 75, May 2023, pp. 37 - 55*
DOI: https://doi.org/10.7186/bgsm75202305

# Influence of *Alstonia Angustiloba* tree water uptake on slope stability: A case study at the unsaturated slope, Pahang, Malaysia

Muhammad Syamsul Imran Zaini[1], Muzamir Hasan[1,*], Muhammad Farhan Zolkepli[2]

[1] Faculty of Civil Engineering Technology, Universiti Malaysia Pahang, Lebuh Persiaran Tun Khalil Yaakob, 26300 Kuantan, Pahang, Malaysia
[2] Faculty of Civil Engineering, Universiti Teknologi Malaysia, Jalan Iman, 81310 Johor Bahru, Johor, Malaysia
*Corresponding author email address: muzamir@ump.edu.my

**Abstract:** Although previous research has significantly enhanced our understanding of problematic and unsaturated soil behaviour and interaction with structures, there is still an urgent need to address the difficult scenarios that are met with problematic and unsaturated soils. This study examines the effects of tree water uptake at different depths and distances on the improvement of induced water uptakes caused by transpiration via mature *Alstonia Angustiloba* tree. This study is performed to examine the tree water uptake profile in a vegetated slope with the existence of mature *Alstonia Angustiloba* tree at the top and the stability of the slope during various precipitation penetration events by which the data of the tree water uptake produced within this section of the slope is recorded and implemented to evaluate the factor of safety (FOS). Slope stability analysis is further conducted to explore how plant transpiration affects slope stability. The results indicate that higher tree water uptake lead to the greatest increase of FOS of the slope up to 53% (from 2.17 to 4.57). The highest tree water uptake recorded was at the slope station with *Alstonia Angustiloba* tree with a depth of 0.25 m and a distance of 1.1 m from the tree. The tree water uptake utilized in this study can contribute to a carbon-free and eco-friendly approach which can be implemented globally to prevent slope failures.

**Keywords:** Tropical residual soil, slope stability, tree induced suction, shear strength, engineering properties

## INTRODUCTION

In most nations around the globe, residual soil exists commonly in equatorial locations, where frequent precipitation and mild climate are beneficial to erosion, which culminates in profound residual soil profiles (Schiavon *et al*., 2019; Zaini *et al*., 2019, 2020a). Mineralogical composition and microstructure (Hasan *et al*., 2021a; Zaini *et al*., 2022a; Zaini *et al*., 2023) are the two key factors that might contribute to the distinctive properties of residuals. In this type of soil, geological disasters such as landslides are highly to occur. Avalanche is one of the greatest catastrophic geological disasters found in steep places, that has drawn significant interest in geological and geotechnical engineering investigations (Goh *et al*., 2020; Zaini *et al*., 2020b) due to the considerable economic repercussions (Hasan *et al*., 2021b; Hasan *et al*., 2021c; Zhang *et al*., 2022). Landslide encompasses exterior and downward motions of slope particle formation owing to attraction stress via a range of movements such as collapsing, slipping, running and any amalgamation of the above (Pradhan & Siddique, 2020; Zaini & Hasan, 2023).

Recurrent slope collapse along biological and constructed slopes is of relevance as it endangers lives, inhibits economic development, and degenerates the environment (Chen *et al*., 2013; Awang *et al*., 2021; Zaini *et al*., 2022b). Regional populations, visitors and pilgrims are under continuous risk of different environmental disasters, for instance, seismic activity, avalanches, overflows, deluges, and forest fires (Ishak & Zaini, 2018; Pradhan & Siddique, 2020; Zolkepli *et al*., 2021a). In both the geological engineering profession and academia, the topic of slope stability (Zolkepli *et al*., 2019) has been a focus of inquiry for the last seventy years. Numerous approaches suggested in compliance with the existing computational techniques have been refined to attain matureness and acquired the support of the engineering field (Bastola *et al*., 2020; Zolkepli *et al*., 2021b; Bouzid, 2022). No universally agreed explanation of the factor of safety (FOS) subsists. For most bearing capacity problems, the FOS is commonly determined on the premise of the maximum load-bearing capacity (Wang *et al*., 2021). However, for slope stability calculations, it is more convenient that the FOS is connected to the typical strength characteristics of the soil (Basahel & Mitri, 2017; Oberhollenzer *et al*., 2018; Yue *et al*., 2019).

Verdure is contemplated useful to slope stability not only through mechanized soil fortification (Zolkepli *et al*.,

0126-6187; 2637-109X / Published by the Geological Society of Malaysia.

2018; Zhu & Zhang, 2019) but also through root water uptake (Zhu *et al*., 2018). Throughout the uptaking manner, plant roots assimilate dampness via chemical change and expiration (Rees & Ali, 2012), which, resulted in desiccating the soil encompassing the plant roots (Rees & Ali, 2006) and consequently actuating soil suction (Zhu & Zhang, 2015; Feng *et al*., 2020). The fortification impact of plant roots has been well acknowledged around the world, whereas root-water uptake has not however been completely examined (Ni *et al*., 2018; Liang *et al*., 2020). Root-water uptake is a vital component that significantly influences the temporal-spatial water substance conveyance in shallow verdure soil (Nyambayo & Potts, 2010; Ai *et al*., 2020). Nevertheless, this process and its intelligence with soil are not so much realized owing to the inalienable changeability of root engineering and inherent challenges of perceiving below-ground stream forms (Woodman *et al*., 2020; Zaini *et al*., 2020a). As examined by Ishak *et al*. (2021a, 2021b) soil states (e.g. water powered conductivity and entrance resistance), and sorts of verdure (e.g. root dissemination).

Biddle (2001) has concluded that soil moisture transfer from various species of tree can affect the changes in the pattern of soil deficit contour. He also discovered that regardless of soil types, there are significant changes in soil moisture contour due to the different type of trees. Malaysia is a tropical country with the tropical monsoon rainfall and dry period can reflect the patterns of the soil moisture (Hasan *et al*., 2021d). The result and analysis that will be gained is expected to reveal the effect of tree by correlation with the meteorological data. Root of a tree plays an important role in preventing landslides event to occur either it is by modifying the soil moisture regime via evapotranspiration or providing root reinforcement within the soils (Ishak *et al*., 2021b). To prevent the debris flow and landslides from occurring during an extensive rainy season, the first factor is very important especially in the tropics and sub-tropics country where within a year, the evapotranspiration is high. On the other hand, Ishak *et al*. (2021a) had conducted the same research but on different type of tree and tree location which is at the toe of the slope. He found that through the tree water uptake process at the toe of the slope, the FOS of the slope significantly increase up to more than 60%.

Recently, broad exploratory ponders have been investigated to measure intake enticed by distinctive verdure species amid the evaporation and transpiration process. The universality of root geomorphology is fundamental for evaluating the hydrodynamic execution of stagnated frameworks. In addition, recognizable proof of the pattern of root geomorphology that improves soil water intake viably attracts specific consideration. Thus, this study aimed to investigate and monitor the soil water intake dispensation owing to the tree induced suctions created at the top of the soil slope. The modifications of the soil water intake were analyzed to gain the soil moisture profiles near the tree. In addition, we hypothesized that: 1) soil matric suction of the *Alstonia Angustiloba* tree may contribute to enhancing the stability of the tropical residual slope; 2) the moisture variation or the matric suction has been altered via transpiration process in a tropical residual soil slope, and; 3) the tree induced suction may affect the factor of safety (FOS) projected to different weather conditions. Thereby, the goals of the current study were to 1) ascertain soil matric suction at a slope with a mature tree existing at the top of the slope, 2) establish a soil water intake contour dispensation at the active root zone of the tree and; 3) analyze the effect of tree induced suction on factor of safety (FOS) at the chosen slope.

## EXPERIMENTAL DESIGN AND MEASUREMENTS

### Description of study site

Figure 1 illustrated the location of the study conducted. As illustrated in the figure, the tropical residual soil slope with the existing *Alstonia Angustiloba* mature tree is situated in Pahang, Malaysia (3° 48' 45.36"N, 103° 19' 32.16"E). The tropical residual slope studied is uniform and appears to be a cut slope. The area of the slope was about 15 m wide (measured across the slope) and 3 m height (measured down to the slope) with a single mature tree *(Alstonia Angustiloba)* which was located at the top of the slope

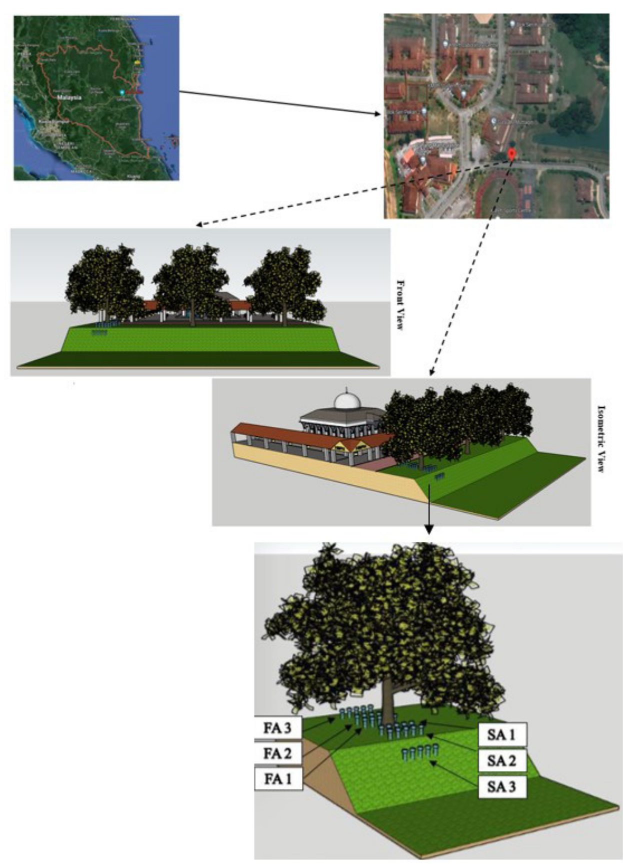


**Figure 1:** Location of field monitoring of the tree water uptake.

with the tree height reaching up to 11 m. There is a total of thirty (30) tensiometers installed in the study area with thirty (3) gypsum blocks to measure the suction of the tree.

### Determination of physical properties of the tropical residual soil

There are three (3) physical properties investigated in this study which comprises of particle size distribution, Atterberg limit, and specific gravity. The particle size distribution for fine-graded soil passing sieve size 63 µm was performed according to ASTM D6913-04 for sieve analysis and ASTM D7928 for hydrometer analysis. Besides, by using the cone penetration or the cone penetrometer method, the Atterberg limit test was conducted according to ASTM D4318-17. The specific gravity of tropical residual soil was examined by carrying out the small pycnometer test by referring to ASTM D792-20. The specific gravity is calculated by using Eq. 1.

$$G_s = \frac{(m_2 - m_1)}{(m_4 - m_1) - (m_3 - m_2)} \qquad (1)$$

Where $m_1$ is the mass of the empty pycnometer, $m_2$ is the mass of the pycnometer with dry soil, $m_3$ is the mass of the pycnometer with soil and water, $m_4$ is the mass of the pycnometer and water and $G_s$ is the specific gravity. The experimental setup for the physical properties of tropical residual soil is shown in Figure 2(a).

### Determination of shear strength parameters of the tropical residual soil

The calculation of bulk and dry density ($\rho_b$ & $\rho_d$) and moisture content ($\omega$) of the soil sample was performed before Consolidation Isotropic Undrained (CIU) test. The test was conducted based on the techniques described in ASTM D7263-21 to acquire the correlation between moisture content with dry density. Figure 2(b) demonstrates the experimental setup in determining the shear strength of the tropical residual soil.

Three (3) soil samples (38 mm diameter with 76 mm height) using a simple soil splitter were prepared to perform the Consolidated Isotropic Undrained (CIU) triaxial compression test as shown in Figure 2(b). Various confining pressures of 100 kPa, 150 kPa, and 200 kPa to determine both saturated ($c'$, $\varphi'$) and unsaturated ($\varphi^b$) shear strength parameters via GDS Fully Automated Triaxial System (GDSTAS) were conducted. The CIU triaxial compression test was conducted in order to acquire the shear strength

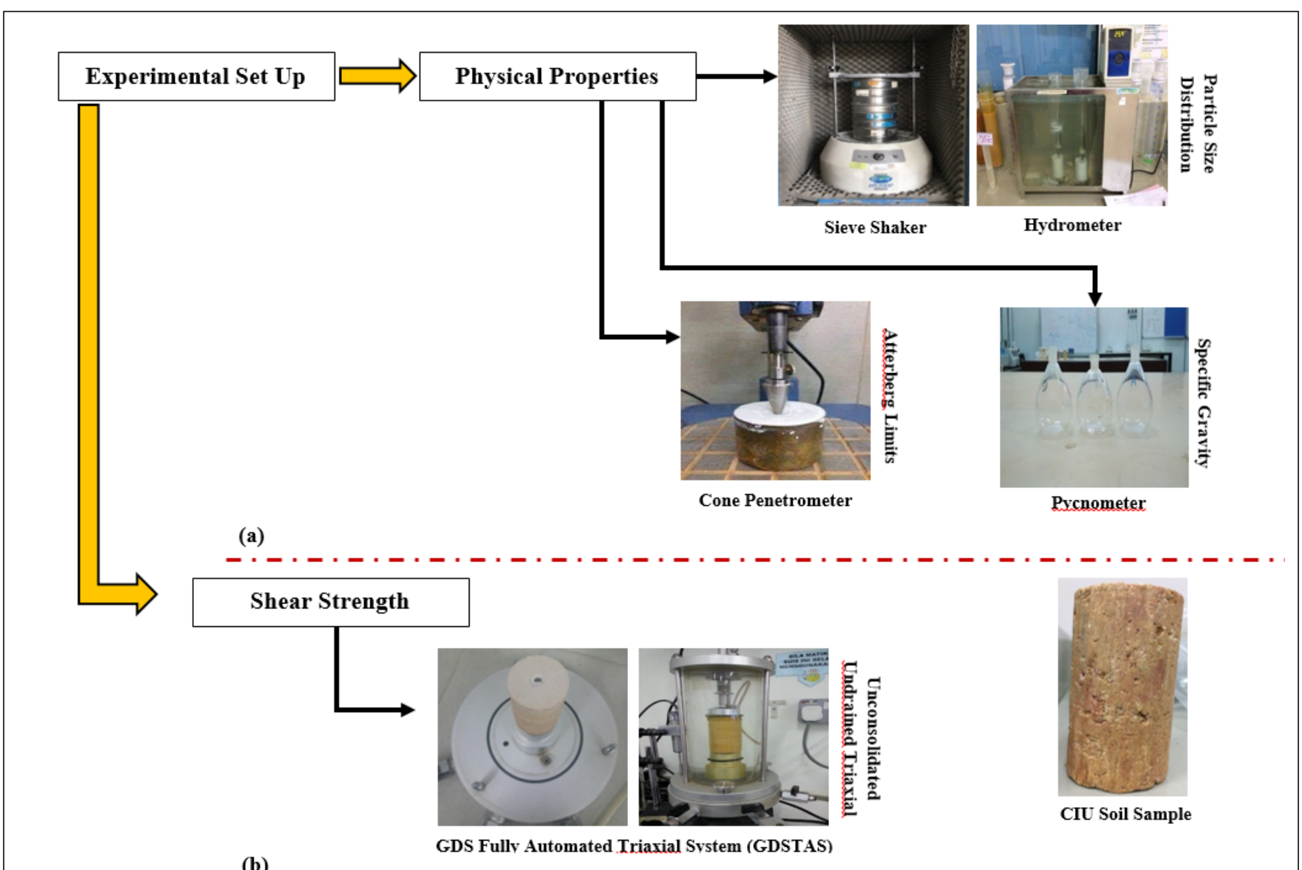


**Figure 2:** Experimental setup in determining: a) physical properties of tropical residual soil; and, b) shear strength parameter of tropical residual soil.

under different confining pressure for the tropical residual soil. Based on Ishak *et al*. (2021a), in Malaysia, the CIU test is more suitable for examining the shear strength parameters of the soil owing to most of the soil being in consolidated and undrained condition. The CIU triaxial compression test was performed according to ASTM D4767.

### Field monitoring work

The tensiometers and gypsum moisture block were used to evaluate the water uptake in soil which is less than 100 kPa and more than 100 kPa respectively. A combination of tensiometers and gypsum moisture blocks was utilized to evaluate the tree water uptake in exploration to view the considerable matric suction induced by the transpiration process. In this study, six (6) stations of tensiometers and gypsum moisture blocks were placed at the slope area and at the flat area, namely as Slope Area 1 (SA 1), Slope Area 2 (SA 2) and Slope Area 3 (SA 3) together with Flat Area 1 (FA 1), Flat Area 2 (FA 2) and Flat Area 3 (FA 3) as shown in Figure 1. Each station consists of a top, middle and bottom of the root zone to monitor the profle of the matric suction changes in both areas (Kardani *et al*., 2021; Ishak *et al.*, 2021b). Figure 4 shows the calibration and capability of tensiometer and gypsum block.

According to Zaini *et al*. (2020a), each station of tensiometers was located at a distance of 1.1 m (0.1h), 2.2 m (0.2h) and 4.4 m (0.4h) from the tree. The distance of the tensiometers was set based on the height of the tree (h = 11.0 m). Therefore, the distance from the tree for each area (Slope Area and Flat Area) were 1.1 m, 2.2 m and 4.4 m from the tree trunk and were embedded vertically in the soil down to the depth of 0.25 m, 0.5 m, 1.0 m, 1.5 m and 2.0 m as shown in Figure 3.

The gypsum block (Delmhorst Instrument Co. Model 5KS-D1 G-Block) was utilized owing to measure the higher range of suction which is beyond 100 kPa up to 1000 kPa. A total of thirty (30) units of the instruments were installed at different depths which were at 0.25 m, 0.5 m, 1.0 m, 1.5 m and 2.0 m at the vicinity of the trees at the top of the slope to measure the in-situ soil matric suction. Each station (FA 1, FA 2, FA3, SA 1, SA 2 and SA 3) was installed with five (5) gypsum blocks considered as the top, middle and bottom of the root zone according to Biddle (2001) and the active root zone were assumed has extended until to a depth of 2.0 m.

The Jet-fill Tensiometer Model 2725 with a total number of thirty (30) units were installed at different depths which were at 0.25 m, 0.5 m, 1.0 m, 1.5 m and 2.0 m to measure the in-situ soil matric suction. Biddle (2001) and Rees & Ali (2012) measured the moisture content and changes of moisture content in the tree proximity by using a neutron probe and found that the influence of the plant root was intensively related to the depth of not more than 2.0 m. Hence, it is assumed that the set-up tensiometers at the greatest deepness of 2.0 m should be adequate to allow a good evaluation of the alterations in tree water uptake in the study area.

At the corner of about 20 m from the tree in the study area, the bucket of rain gauge was placed on tripod staph. The model of Rainew (see Figure 3) with a current counter-logging rain gauge with a tipping bucket was set up at the study area to evaluate the continuous real-time precipitation rate.

### Determination of soil suction contour at the active root zone

The 2-Dimensional and 3-Dimensional soil matric suction contour was developed via GiD software and Surfer software respectively using the definition of materials, geometry, parameter, solution information and conditions. The software generates a mesh for finite elements and generates details of a mathematical simulation of the typical geometrical slope of the study area. Hence, the field monitoring data monitored for six (6) months were applied in this software and was presented to visualize the results and analysis of the tree water uptake.

### Assessing the slope stability of the unsaturated tropical residual soil slope

Through the commercial software of SLOPE/W version 7.03, 2007, the initial basic checks of the slope stability results were generated and compared to the previous approach equation. Besides, the critical slip surface found by trial and error was also determined using the SLOPE/W software. There are 64 possible failure surfaces that were examined to find the critical slip surface as demonstrated in Figure 5. In the study, to evaluate the weight of the soil bounded utilized to Eq. 2 (Ishak *et al*., 2018; Zolkepli *et al*., 2018), the critical slip surface was separated into fifteen (15) slices. The real slope arithmetic completed with the critical slip surface moved through the top of the slope, the position of each slice and slope elevation were shown in Figure 5.

$$F = \frac{(\sum c'lR + (W \cos \beta) R \tan \phi' + SRl \tan \phi^b)}{(\sum WR \sin \beta)} \tag{2}$$

Where, $c'$ is the cohesion, $l$ is the slip arc length, R is the radius of circular failure surface (m), W is the surcharge load (kN), β is the angle between the tangent to the centre of the base of each slice and the horizontal, $\phi'$ is the internal friction angle of the saturated soil and $\phi^b$ is the internal friction angle of the unsaturated soil.

The lowest FOS of 1.868 was evaluated by using SLOPE/W software through the traditional method of slices. To examine the differences and percentage differences of FOS with other selected methods, the FOS of 1.868 was utilized as a referenced value. This specific slip surface coincides with a radius of 3.88 m and origin x = 5.00 m, y = 7.88 m from the marked point at the studied tropical residual soil slope. The result acquired for this specific

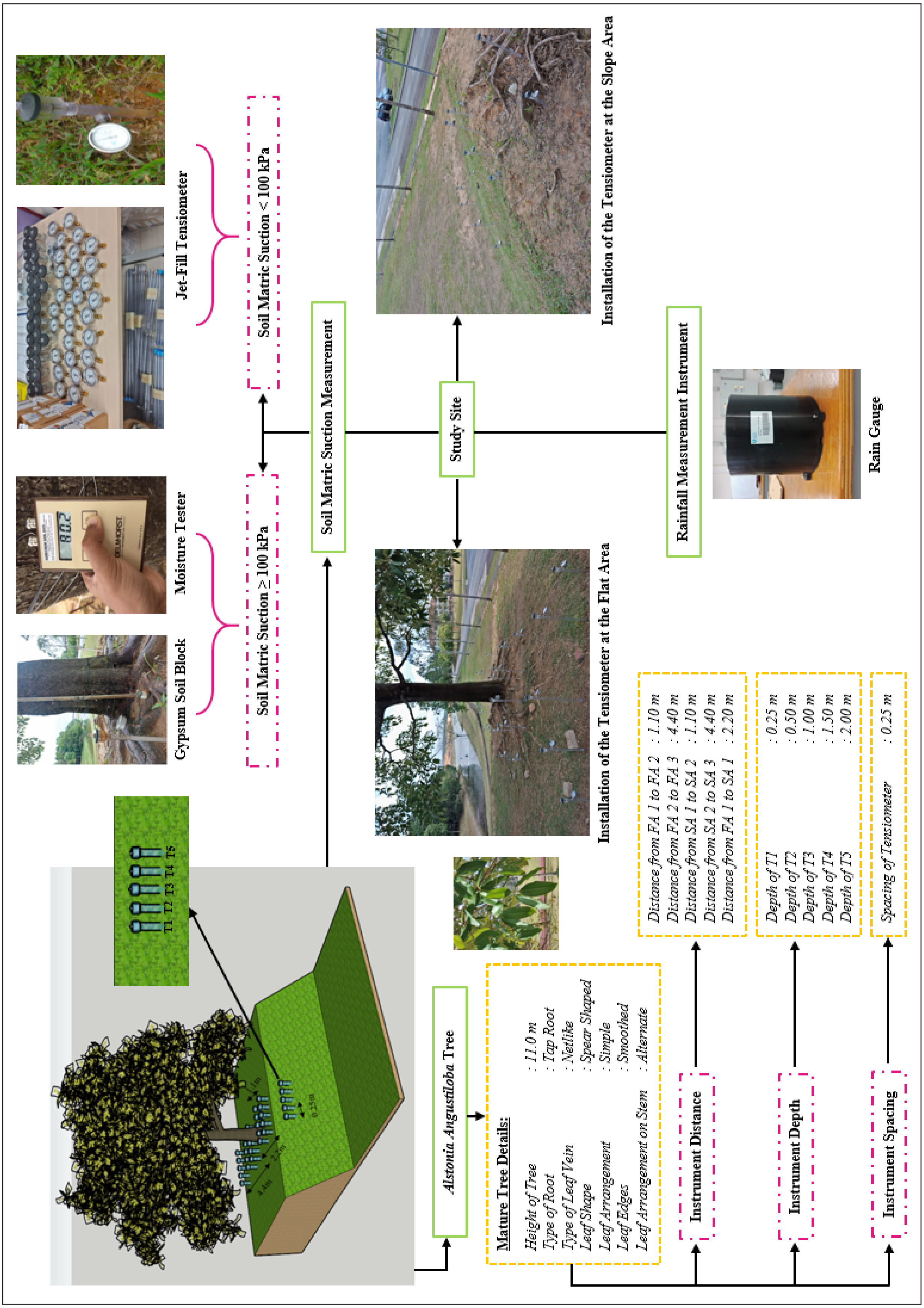


**Figure 3:** Experimental setup in determining the soil matric suction and rainfall intensity.

slip surface were implemented from Eq. 2 in contrast to the multiple approaches accessible in SLOPE/W software. Figure 5 shows the variations between various approaches ranging from 1% to 4% in contrast to the manual evaluation. The difference between the Eq. 2 and the Ordinary method (Fellenius Method- SLOPE/W) usage was small owing to the fact that these two (2) methods were adopted from a very similar formula in approach and equation.

### Statistical analysis

Numerical interpretations were performed using Microsoft Excel 2010. One-way analysis of variance (ANOVA) was conducted to collate the rainfall intensity and the soil matric suction. Fisher's least significant difference (LSD) was used to identify significant differences between means separation at a level of $p< 0.05$. Furthermore, Pearson's correlation analysis was used to determine the correlations between the rainfall intensity, distance of tensiometers from the tree, depth of the slope and station area. The error bars were used to indicate whether the results obtained are significantly different as discussed in detail in the following section.

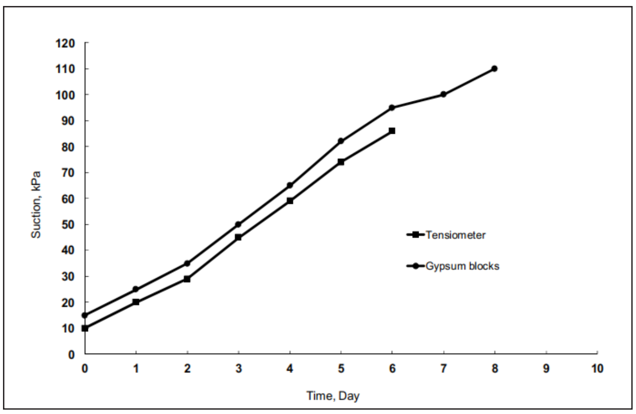


**Figure 4:** Calibration and capability of tensiometer and gypsum block.

## RESULTS AND DISCUSSION

### Physical properties of tropical residual soil

The main physical property performed in this study comprises sieve analysis, Atterberg limits, and specific gravity. According to the British Soil Classification System (BSCS), the tropical residual soil was categorized as having very high plasticity of sandy SILT (MVS) soil. The result of sieve analysis from a portion of 100 g soil specimen comprises 4.2 % greater than 2 mm (gravel), 27.9 % within the size of 2 mm to 0.063 mm (sand), 45.1 % within 0.063 mm to 0.002 mm (silt), and 22.8 % is lower than 0.002 mm (clay). Figure 6 demonstrates the particle size distribution of the tropical residual soil for the unsaturated slope studied. Besides, the Atterberg Limit of tropical residual soils from the study area suggested that the liquid limit (LL) of the soil was 70.0 %, the plastic limit (PL) was 31.0 % and the Plasticity Index, (PI) was 39.0 %. According to the British

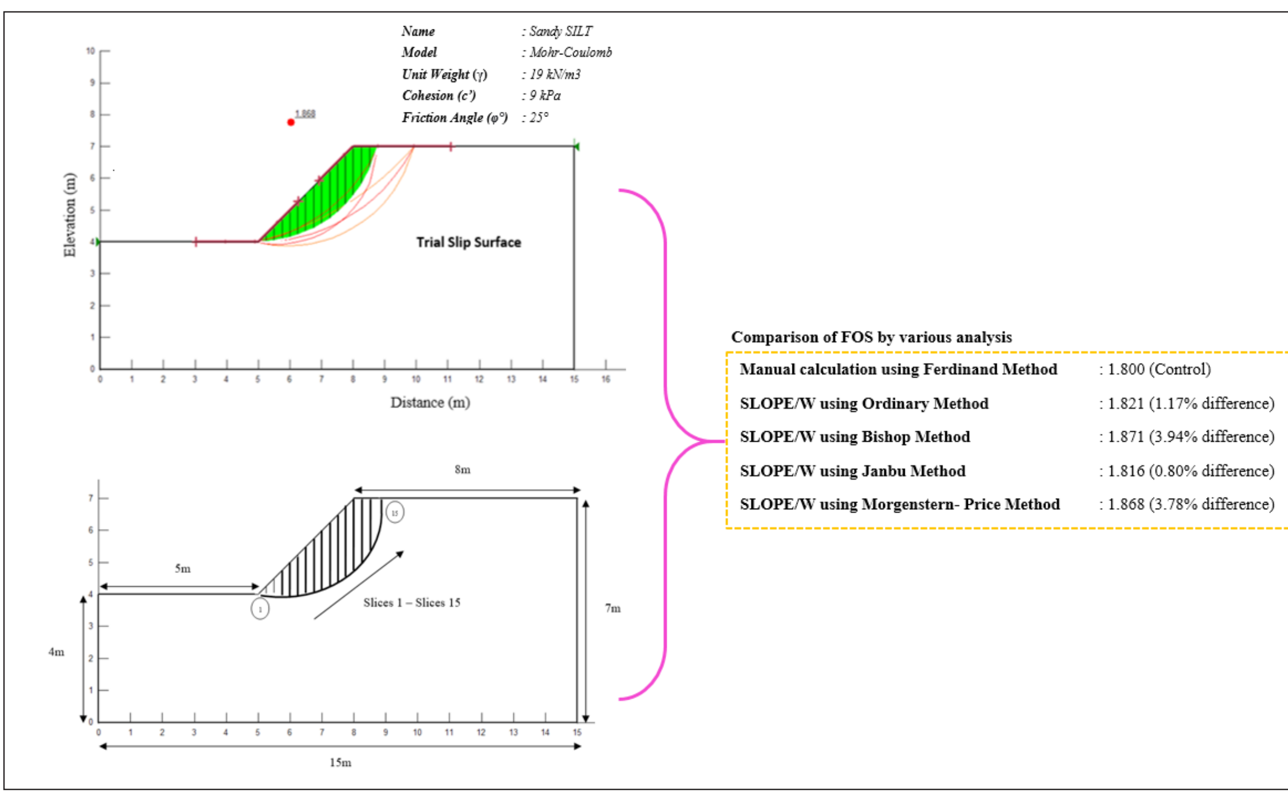


**Figure 5:** Slope geometry of the tropical residual soil with the comparison of FOS by various analysis.

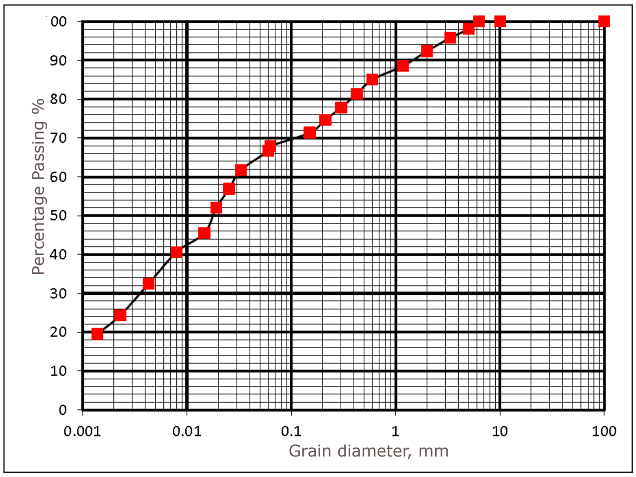


**Figure 6:** Particle size distribution graph of tropical residual soil.

Soil Classification System (BSCS), the soil at the site study at the field can be categorized as SILT of high plasticity (MHS) with a relative density of 2.74. As stated by Zaini *et al*. (2020a), owing to a wide modification of metallurgy, the relative density of tropical residual soils is commonly low or uncommonly high. The physical properties values obtained in this study are coherent with the investigation performed by Ishak *et al*. (2021a) and Zolkepli *et al*. (2018).

## Unsaturated shear strength of tropical residual soil

As reported by Ishak *et al*. (2021b), the latest criterion presented was the unsaturated friction angle, $f^b$ which is always smaller than or equivalent to the saturated friction angle, $f'$. Rees & Ali (2012) deduced the shear strength of soil is rectilinearly proportionate to the tree water uptake (where $f^b$=$f'$), where the tree water uptake is smaller than the air-entry value. Table 1 shows the experimental shear strength values of unsaturated soil friction angle, $f^b$ at multiple places in Peninsular Malaysia including the studied unsaturated friction angle, $f^b$ of the tropical residual soil. Based on Table 1, the unsaturated friction angle, $f^b$ was assumed lower than or equivalent to the saturated friction angle, $f'$ (Rahardjo *et al*., 2004; Huat *et al*., 2005; Zolkepli *et al*., 2018; Zaini *et al*., 2020a; and Ishak *et al*., 2021a).

An investigation performed by Fredlund *et al.* (1996) explained that the value of the unsaturated friction angle, $f^b$ is lower or equivalent to the saturated friction angle, $f'$ at a lower or high value of tree water uptake, the value of the unsaturated friction angle, $f^b$ will decrease to a lower value. More water will expel out from the pores of the soil with no further increase of net stress when the matric suction increases (Ishak *et al*., 2021a). Figure 7 illustrates the Mohr's Circle and the effective stress failure envelope for samples 1, 2 and 3. Based on Figure 7, the effective friction angle ($f'$) and the effective cohesion ($c'$) are 25$^o$ and 9 kPa respectively.

## Effects of single respond event to the soil suction distribution pattern of the tropical residual soil slope

### Effects of intense rainfall on the soil suction distribution pattern of the tropical residual soil slope

Researchers such as Biddle (1979), Fredlund *et al*. (1996) and Ishak & Zaini (2018) investigated the response of tree water uptake dispensation owing to a single rainfall pattern on the slope with further diminishing the secular period in the examination. The central to their investigation was insulating precipitation patterns during observation time intervals as multiple precipitation patterns were signified by intense precipitation and prolonged precipitation. Coherent to that, the tree water uptake dispensation patterns for the tropical residual slope without the existing mature tree and with the existing *Alstonia Angustiloba* mature tree were displayed as

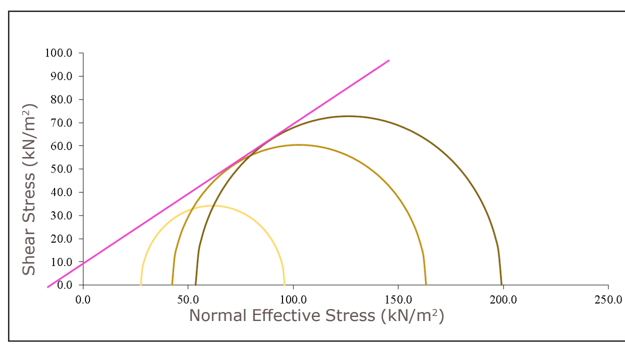


**Figure 7:** Mohr's Circle and the effective stress failure envelope of tropical residual soil.

**Table 1:** Experimental values of unsaturated friction angle, $f^b$ of the tropical residual soil at various locations in Peninsular Malaysia.

| Researcher | Location | $f'$ ($^o$) | $f^b$($^o$) |
|---|---|---|---|
| Zaini *et al*. (2022) | Pahang | 25 | 21 |
| Ishak *et al.* (2021a) | UTM | 23 | 20 |
| Zaini *et al*. (2020a) | Pahang | 25 | 20 |
| Zolkepli *et al.* (2018) | Pahang | 25 | 17 |
| Huat *et al.* (2005) | Sepang | 26 | 26 |
| Rahardjo *et al.* (2004) | Singapore | 25.1 | 24.3 |

per findings performed by the previous researcher with a further comparison of the slope with and without a tree at the top of the slope. The explanation of the precipitation pattern of intense rainfall occurred subsequent to a prolonged dry period. From February 2022 to March 2022, the slope without trees faced the driest states throughout the site observation period which was without any rainfall for ten (10) days. The highest suction recorded at the depth of 0.25 m, 0.5 m, 1.0 m, 1.5 m and 2.0 m were 60 kPa, 62 kPa, 62 kPa, 64 kPa and 66 kPa respectively. These results show that the greatest tree water uptake value by the tropical residual soil is 66 kPa, even during the protracted dry period. However, a normal intense and short tropical precipitation that took place on 24th February 2022 induced the tree water uptake at 0.25 m to 2.0 m depth to dramatically fall to the lowest value as demonstrated in Figure 8.

Figure 8(a) shows the plotted of mean tree water uptake with profiles at slope without tree, demonstrating that substantial tree water uptake can establish during protracted desiccated time intervals even though the tree water uptake has been immediately dissipated with the occurrence of short and intense precipitation events. However, the worst pore-water pressure states did not reach positive pressures at all deepness. The mean tree water uptake profile with depth at slope without tree highlighted that substantial tree water uptake has been readily dissipated with the events of the precipitation with a value of 8.4 mm on 24th February 2022. The suction pattern at 0.25 m, 0.5 m, 1.5 m and 2.0 m depth dropped to the minimum value of 14 kPa, 18 kPa, 26 kPa, 36 kPa and 45 kPa respectively. For a prolonged dry period with sudden intense rainfall events continuously for about ten (10) days without any precipitation, the greatest tree water uptake was observed at the top of the unsaturated slope with the presence of *Alstonia Angustiloba* tree at a depth of 0.25 m, 0.5 m, 1.0 m, 1.5m and 2.0 m were 110 kPa, 96 kPa, 90 kPa, 84 kPa and 66 kPa respectively. The results show that the greatest tree water uptake value of the soil is 110 kPa. The mechanism of high matric suction was identical to the matric suction condition recorded during the prolonged dry period which will be discussed later. Eventually, pursued by the intense precipitation event, the tree water uptake fell but did not achieve the lowest value of tree water uptake at the slope without a tree.

The tree water uptake at the deepness of 0.25 m and 0.5 m dropped from 110 kPa to 84 kPa and from 96 kPa to 80 kPa respectively, while it dropped uniformly at the depth of 1.0 m from 90 kPa to 88 kPa. Subsequently, the matric suction at 1.5 m and 2.0 m depth dropped to a small value only which were from 84 kPa to 79 kPa and from 66 kPa to 60 kPa respectively. The suction at depths 0.25 m and 0.5 m were delicate to intense precipitation events compared to the depth of 1.0 m, 1.5 m and 2.0 m which were not greatly affected. Although both of the slopes obtained an equal quantity of precipitation but the variation responses in tree water uptake value can be certainly demonstrated at a slope with a tree at the top (See Figure 8(b)).

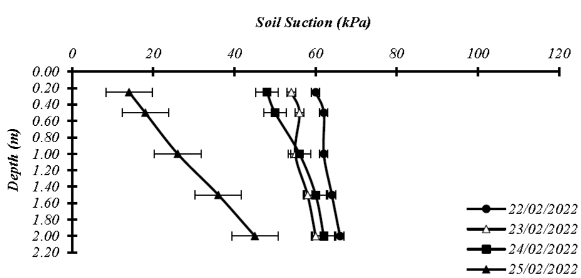


(a)

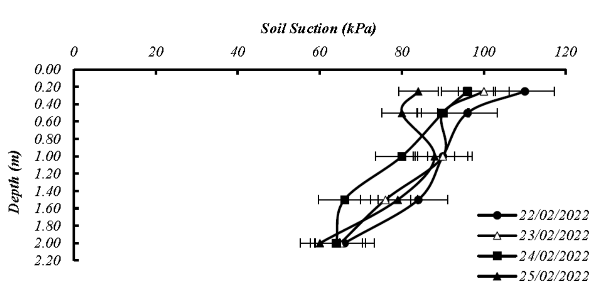


(b)

**Figure 8:** Soil matric suction with respect to the intense rainfall precipitation at: a) slope without the tree; b) slope with *Alstonia Angustiloba* mature tree.

### Effects of antecedent rainfall on the soil suction distribution pattern of the tropical residual soil slope

The tree water uptake demonstrated periodic variation during desiccated time intervals mainly due to the periodic variation in solar emission during day and night. The result insinuates that other than the precipitation penetration, the earth's surface surrounding such as the breeze, climate, dampness and solar emission could alter the tree water uptake as well. When both of the slopes received moderate rainfall on 18th April 2022, the suctions at 0.25 m down to 1.5 m dropped gradually while the suction at 2.0 m dropped not as greatly as other depths. Figure 9(a) and 9(b) show the tree water uptake profiles on the tropical residual slope with and without trees as a result of antecedent precipitation. The tree water uptake at 2.0 m was only altered by the intense rainfall that occurred on 20th April 2022. The results suggested that the arrangement of the rainfall act as a crucial parameter in the propagation of infiltration of water on both slopes. Both profiles also revealed that the continuous low intensity of rainfall that occurred from 17th April 2022 to 18th April 2022 has no significant effect in reducing the matric suction. In the period of the antecedent rainfall pattern, the lowest suctions were encountered at 0.25 m, 0.5 m and 1.0 m on 19th April 2022. Nonetheless, the antecedent rainfall from 18th April 2022 to 19th April 2022 on both slopes shows significant effects on the distribution of the suction.

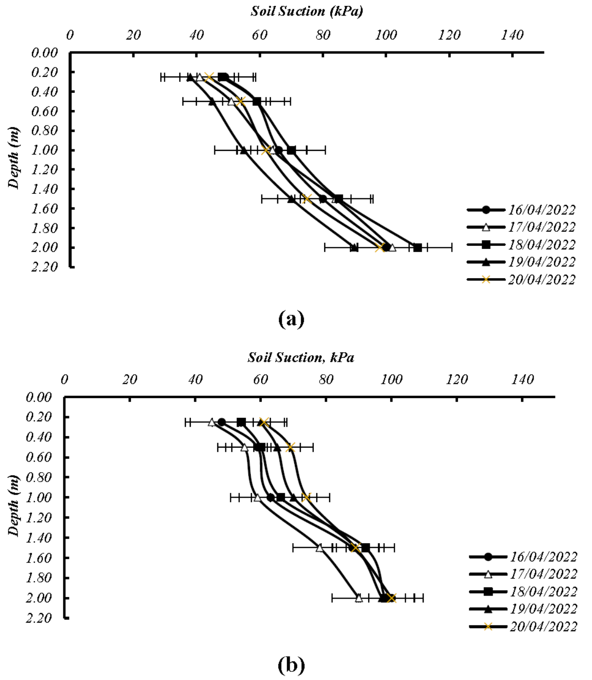


**Figure 9:** Soil matric suction with respect to the antecedent rainfall precipitation at: a) slope without the tree; b) slope with *Alstonia Angustiloba* mature tree.

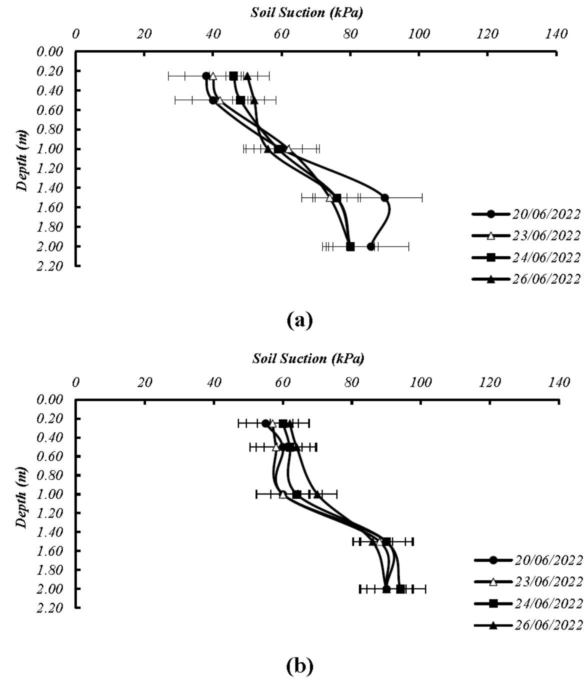


**Figure 10:** Soil matric suction with respect to the prolonged antecedent rainfall precipitation at: a) slope without the tree; b) slope with Alstonia Angustiloba mature tree.

Additionally, the comparison of the rainfall pattern illustrated in Figure 9 shows a good agreement of suction distribution pattern in the period of rainfall pattern in both slopes has been achieved. It can be summarized that a canopy interposing was trivial owing to the moderately and antecedent intense quantity of precipitation that occurred and there was no significant difference in terms of the tree water uptake between the slope with a tree at the top and the slope without a tree (Hongde *et al*., 2021).

## Effects of prolonged antecedent rainfall on the soil suction distribution pattern of the tropical residual soil slope

In the period of continuous daily rainfall from 20th June 2022 to 26th June 2022 for both of the slopes, owing to the greater precipitations, the tree water uptake was substantially diminished as demonstrated in Figures 10(a) and 10(b). Based on the amalgamation of intense and antecedent precipitation, the lowest tree water uptake at 0.25 m, 0.5 m and 1.0 m were encountered on 23rd June 2022 due to the highest rainfall amount on 20th June 2022 (60 mm/day). From the results, it can be summarized that the lowest tree water uptake in the soil in both of the tropical residual soil slopes in the study area was controlled by the precipitation intensity jointly with the antecedent precipitation. At all depths, the worst pore-water pressure did not reach the saturated state which was at 0 kPa value. Therefore, the canopy interposing was trivial owing to the event of moderately and antecedent intense quantity of precipitation which allowed rainfall to blow on the soil under the canopy of the tree *(Alstonia Angustiloba)*.

During the wet period which was at prolonged and antecedent rainfall, the matric suction decreased due to the high precipitate of water in the soil. At this condition, the results show no substantial variations between matric suction within the proximity of the tree and without the tree at the slope. During the no rainfall period, the matric suction on the slope without a tree increased slower compared to the slope with a tree at the top. Moreover, the preserved mature tree *(Alstonia Angustiloba)* would expedite the tree water uptake and serve as an effective method to reduce soil moisture. During the dry period, the matric suction within the vicinity of the tree was remarkably higher than the tree water uptake subjected to the distance of the mature tree. The dry soil with high matric suction would lead to an increment of soil strength within the proximity of the mature tree.

## Effects of prolonged dry condition on the soil suction distribution pattern of the tropical residual soil slope at different stations

The response of suction distribution of various rainfall patterns during eight (8) months of field monitoring at the study area shows that the soil lost its moisture intake regularly after undergoing normal minor and major precipitation events. The intense and short precipitation and precipitation amount tend to be one of the leading factors to the water intake alteration at a slope without a tree but not at a slope with a tree at the top. The tree canopy can be a component to effect the tree water uptake alteration at the slope with the tree as the canopy interposing will diminish the amount of precipitation infiltration into the soil. The antecedent and prolonged rainfall were identified as the major dominant factor to a suction variation on both of the slopes (with and without trees) in the study area. In the period of this field monitoring, a period without rainfall was encountered from 13th February 2022 to 22nd February 2022. These conditions were recorded to represent the tree water uptake profile at all locations which were at SA 1, SA 2, SA 3, FA 1, FA 2 and FA 3. Coherently, the tree water uptake profiles right after the antecedent and prolonged precipitation on both slopes which were at slope without a tree and slope with a tree at the top were recorded as presented in Figures 11(a) and 11(b). The data collected on 13th February 2022 was identified as the lowest matric suction value which was determined as the initial condition.

Figures 12(a) and 12(b) show the results on 18th February 2020 of the continuing increment value of matric suction after ten (10) days without rainfall. Due to the exposure to the dry period, the tree water uptake at the top of 2.0 m depth has greatly increased. In addition, the highest matric suction was encountered at SA 1 and FA 1 at the deepness of 0.25 m and 0.5 m respectively with a value of 66 kPa,

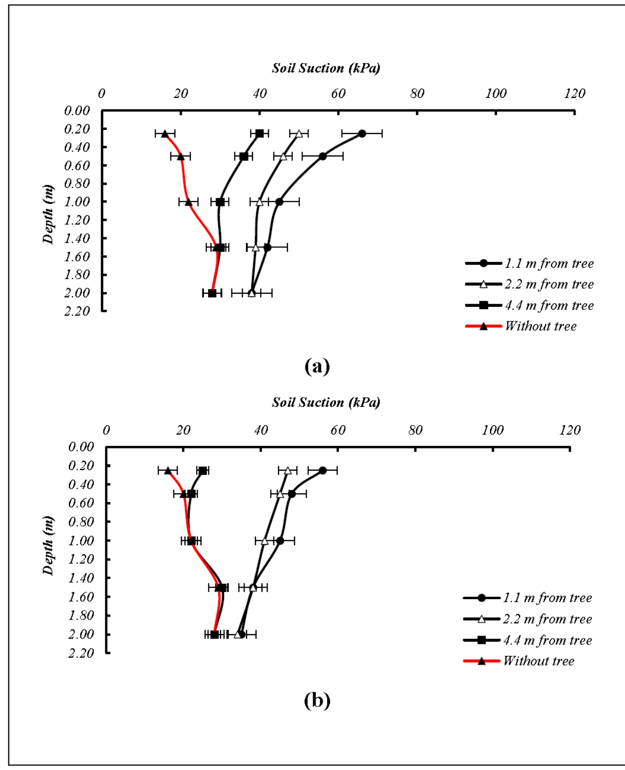


**Figure 12:** Soil matric suction with respect to the prolonged dry condition on 18th February 2022 in: a) slope area; b) flat area.

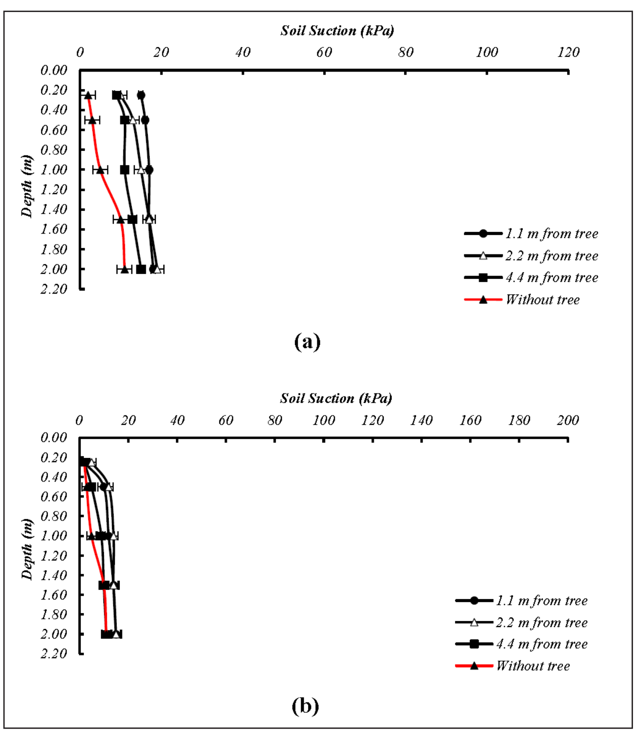


**Figure 11:** Soil matric suction with respect to the prolonged dry condition on 13th February 2022 in: a) slope area; b) flat area.

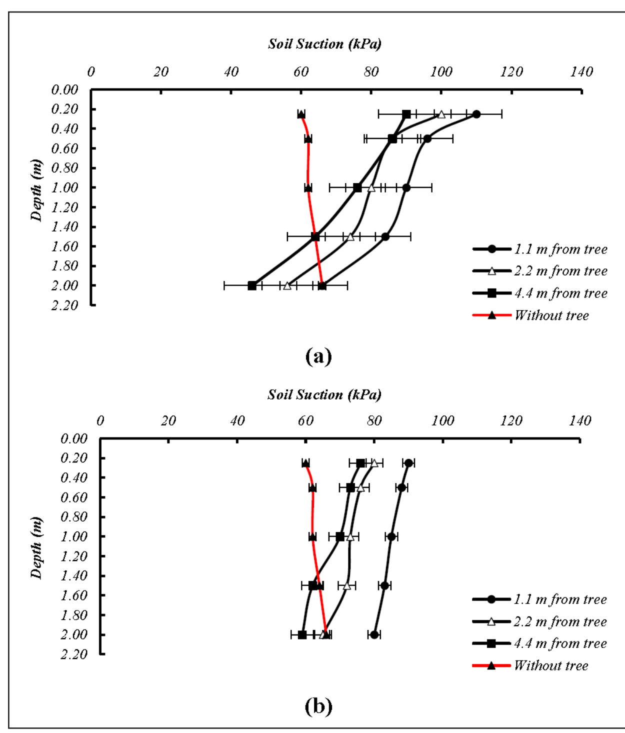


**Figure 13:** Soil matric suction with respect to the prolonged dry condition on 22nd February 2022 in: a) slope area; b) flat area.

56 kPa; and 56 kPa, 48 kPa respectively compared to the slope without a tree.

The data collected on 22nd February 2022 illustrates in Figures 13(a) and 13(b) show the maximum value of the tree water uptake during the desiccated condition. The changes in tree water uptake dispensation arrangements were produced in various states. After ten (10) days without rainfall, the tree water uptake at the top of 2.0 m increases constantly to the right. Besides, the tree water uptake at 1.1 m from the *Alstonia Angustiloba* mature tree at SA 1 and FA 1, particularly at the deepness of 0.25 m and 0.5 m were higher than at slope without the *Alstonia Angustiloba* mature tree with a matric suction of 110 kPa and 96 kPa (SA 1) and 90 kPa and 88 kPa respectively (FA 1).

The comparison of the matric suction between the slope with a tree at the top and the slope without a tree was done by the previous researcher such as Zhu & Zhang (2015) and Feng *et al*. (2020). Based on the investigation performed by the previous researchers, the tree water uptake created in bare and vegetated soil columns in the site and physical prototype in the soil laboratory yielded a result that proved 100% of tree water uptake produced in the stagnated pillar was greater than the barren soil pillars. Coherent to that, the evaluated tree water uptake at the slope without a tree was ascribed to the evaporation process which was lowered than at the slope with a tree at the top as it was engendered by the transpiration process. As clearly shown in Figures 13(a) and 13(b), the dispensation of the tree water uptake at 1.1 m from tree was significantly greater than the tree water uptake at 4.4 m from the tree and with the slope without a tree. The comparison of the matric suction distribution at SA and FA for both 13th February 2022 and 22nd February 2022 demonstrates that the tree water uptake at SA was higher than FA owing to the growth of active roots in a lateral position that the underneath growth with better focused at SA (Ishak *et al.*, 2021b).

### Representation of field monitoring at the tropical residual soil slope corresponding to the various rainfall events

The model of slope illustrated in Figure 14 consists of 86 elements of quadrilateral mesh with 90 nodes for the 2D model generated using GiD software and 120 nodes for the 3D model using Surfer software. The matric suction was presented according to the mesh and nodes in revealing a typical drying pattern or soil moisture deficit which was considered as moisture migration effected by a single mature tree at the top of the slope. By assuming the root region to an extent of 2.0 m depth and a radiated distance of 4.4 m symmetrical for both right and left from the focal point of the tree. The consideration of the root region extends laterally and beneath the top of the slope. Hence, some drying patterns with high matric suction from the top of the tree to the slope crest can be expected from this situation. At 0.25 m and 0.5 m depth of antecedent rainfall, the lowest water uptake recorded were 56 kPa and 60 kPa on 13th February 2022 respectively. The volume of rainfall penetration on the sloping surface was small owing to the water runoff.

The field monitoring result of 18th February 2022 showing an increment in tree water uptake produced by the tree water uptake was applied on a mesh model as shown in Figure 14. Figure 14 also revealed that the changes of the tree water uptake modifications or soil moisture loss proximity of the mature tree within the slope have occurred. The figure also showed the presence of the greatest suction of 80 kPa produced at the bottom of the *Alstonia Angustiloba* mature tree at the top of the unsaturated slope in the soil matric suction contour. Figure 15 shows the tree water uptake on 22nd February 2022 which indicated a rapidly developed tree water uptake compared to 18th February 2022. The greatest water uptake value of 110 kPa was greatest at the bottom of the tree at the top of the slope with the lowest water uptake value of 64 kPa. The absence of rainfall for ten (10) days has developed the soil suction contour which obviously indicated that the matric suction of the observed slope decreased with the increment of distance from the tree. After several days of the antecedent rainfall event, the soil matric suction remarkably decreased owing to the high amount of rainfall infiltration. From the cycle, the soil matric suction shows a significant increase owing to tree water uptake during the dry period. It can be summarized that the existence of the *Alstonia Angustiloba* tree help to enhance the soil matric suction which increased the level of water expelled from the soil through the active root tree which is coherent with the research conducted by Hongde *et al*. (2021).

### Effects of soil matric suction on the stabilization of the tropical residual soil slope

As highlighted in the previous section, $\phi^b$ angle was one of the parameters that differ with the tree water uptake increment. This parameter is significantly important to influence the overall calculation of the FOS for the slope as shown in Table 2. From Table 2, it can be analysed that the magnitude of $\phi^b$ angle varies with the matric suction increment. As an example, for soil matric suction from saturated condition range to residual water content matric

**Table 2:** Non-linear value of $\phi^b$ angle at several suction ranges.

| Soil Type | $\gamma$, (kN/m³) | At suction 0-80 kPa $\phi^b$, (°) | At suction 80-100 kPa $\phi^b$, (°) | At suction 100-300 kPa $\phi^b$, (°) |
|---|---|---|---|---|
| Sandy SILT | 19 | 20 | 14 | 10 |

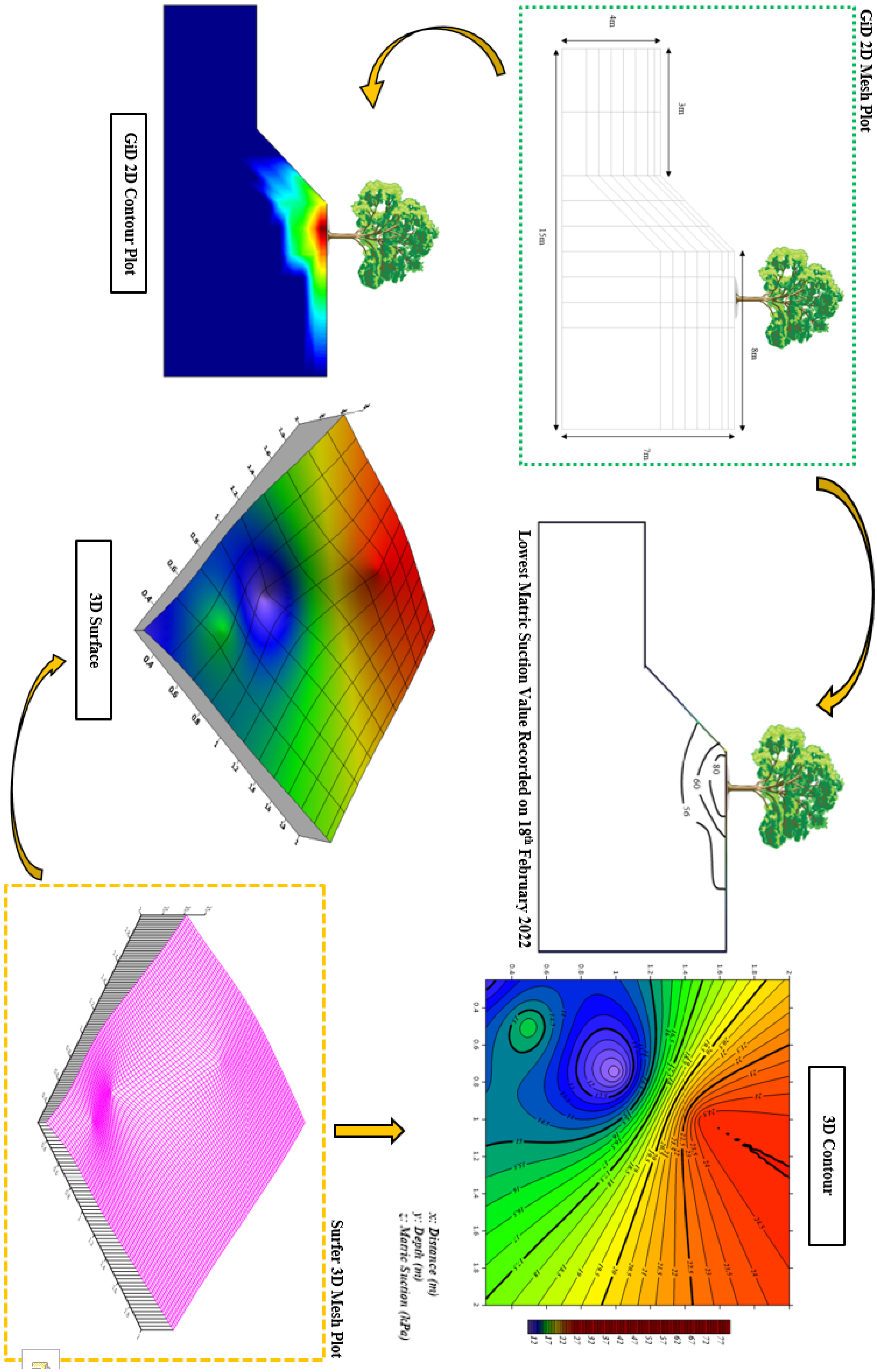


**Figure 14:** Soil matric suction (kPa) contour corresponds to the lowest soil matric suction throughout eight (8) months of field monitoring on the tropical residual soil slope.

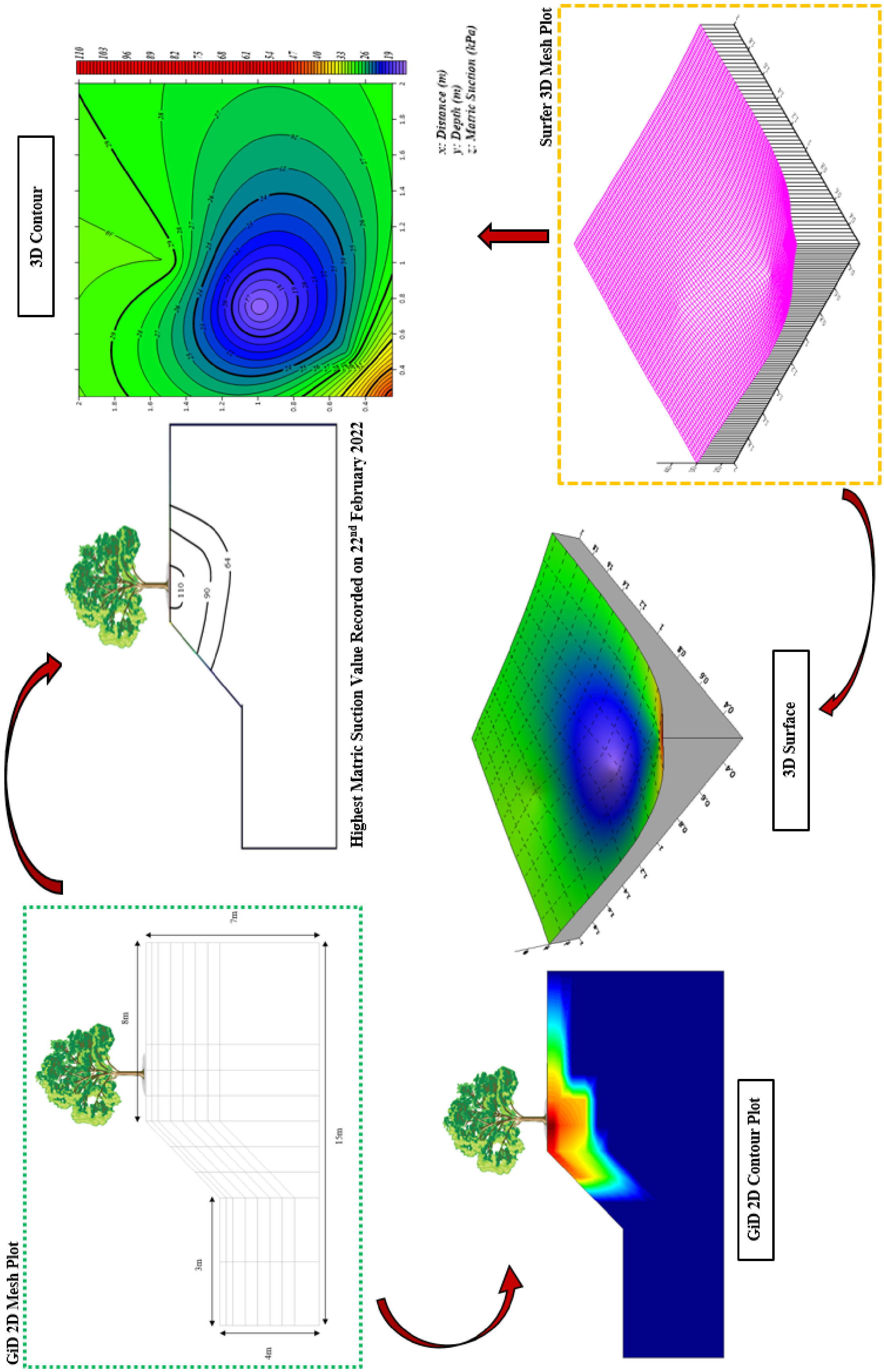


**Figure 15:** Soil matric suction (kPa) contour corresponds to the highest soil matric suction throughout eight (8) months of field monitoring on the tropical residual soil slope.

suction (0-80 kPa), $\phi^b$= 20°, at residual water content matric suction (80-100 kPa) $\phi^b$= 14° and beyond residual water content matric suction (> 100 kPa) $\phi^b$= 10°. Based on the remaining moisture content of matric suction, the soil shear strength envelope shows a constant value beyond the residual water content of matric suction. Figure 16(a) shows how the FOS responds to various matric suction for the values of the $\phi^b$ angle. The increment of FOS was due to the value of matric suction and $\phi^b$ angle increased with almost the same pattern as non-linear variation as indicated in Figure 16(a). The FOS was performed using a matric suction profile which corresponds to the maximum value encountered from the field monitoring program and the calculations of the FOS were performed by using the range of the actual value of matric suction obtained from the field monitoring.

In assessing the actual slope stability in the study area, the matric suction profiles that were presented in the previous section are discussed in this section. The tree water uptake profiles encountered from the site observation work were implemented for FOS calculations. The location of the critical slip surface with slices that were integrated directly with the soil matric suction coherent to the 2D contour plot was illustrated (see Figure 16(b)). The effect of the transpiration process from a tropical mature tree in order to induce the soil matric suction in the vicinity of the tree was used to perform the slope stability analysis through eight (8) months of field monitoring. The field data provided useful information on the soil matric suction changes generated by the drying process of the tropical mature tree at the base of each slice.

Figure 17 demonstrates the modifications in values of the FOS against catastrophe during eight (8) months of site observations which included the combination of rainfall precipitation and FOS data. The relationship of FOS with the tree water uptake of the tropical residual soil from February 2022 to September 2022 was presented in Figure 17. The primary FOS saturated slope was 1.868 which was lowered than the unsaturated slope with the nonexistence of *Alstonia Angustiloba* mature tree and the FOS differ with time and tree water uptake. The increment in FOS trending owing to several shifting upward of the line during the drying period

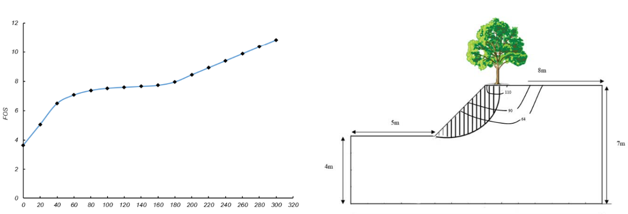


(a) (b)

**Figure 16:** Relationship between a) Proportionality of matric suction with FOS; (b) Matric suction with critical slip surfaces for FOS calculations.

can be clearly seen in Figure 17. These arrangements of drying were separated in various circumstances, initiating in the month of February 2022 to March 2022, May 2022 to June 2022 and July 2022 to September 2022. Within these time intervals, soil moisture loss has taken place on the soil to sustain a high tree water uptake. As the tree water uptake abruptly dropped due to higher precipitation which reduced the FOS through the one-day infiltration process.

Moreover, the increment in FOS value will gradually increase within a time of one (1) to two (2) weeks after the heavy rain events occurred via the evaporation process as demonstrated in Figure 17 (FOS without tree). Coherently, the protection of the tropical tree can greatly enhance the tree water uptake which will affect the stabilization of the unsaturated slope. On 19th February 2022 the FOS of the slope with the *Alstonia Angustiloba* mature tree at the top achieved up to 53% greater than the FOS of the slope without the existence of the *Alstonia Angustiloba* mature tree. The increment of the tree water uptake on the slope with the *Alstonia Angustiloba* mature tree at the top substantially enhanced the stability of the unsaturated slope compared to the slope with the absence of the *Alstonia Angustiloba* mature tree. The existence of the tropical mature tree has a great effect in accelerating the tree water uptake after the rainfall event and acts as a practical tool to eliminate water from the tropical residual soil which can directly poise the tropical residual soil slope.

### Statistical analysis via standard error, analysis of variance (ANOVA), Fisher's Least Significant Difference (LSD) and Pearson's Correlation Coefficient

The error bars indicate the standard error of the parameters observed in this study. The error bars were evaluated based on the overlapping bars between the data and the length of the error bars within the same and different groups (at $p < 0.05$) of studies (see Figure 8 to Figure 13 and Figure 17) coherent to the investigations made by Hasan *et al*. (2021a) and Zaini *et al.* (2022). The overlapping error bars indicate the insignificant differences between the data while the data that is not overlapped indicates the significant differences in the data. Based on Figure 8(a), at the unsaturated slope without a tree with respect to the intense rainfall, the soil matric suction on 25th February 2022 at various depths shows significant differences with the soil matric suction on 22nd February 2022 to 24th February 2022 as the error bars at different depth is not overlapped with each other. However, there are insignificant differences between the soil matric suction on 22nd February 2022 to 24th February 2022 as the error bars overlapped with each other at the depth of 1.0 m to 2.0 m. There is a smaller difference between the soil matric suction between 22nd February 2022 to 24th February 2022 at the depth of 0.25 m and 0.50 m. At the unsaturated slope with the existence of *Alstonia Angustiloba* mature tree, the soil

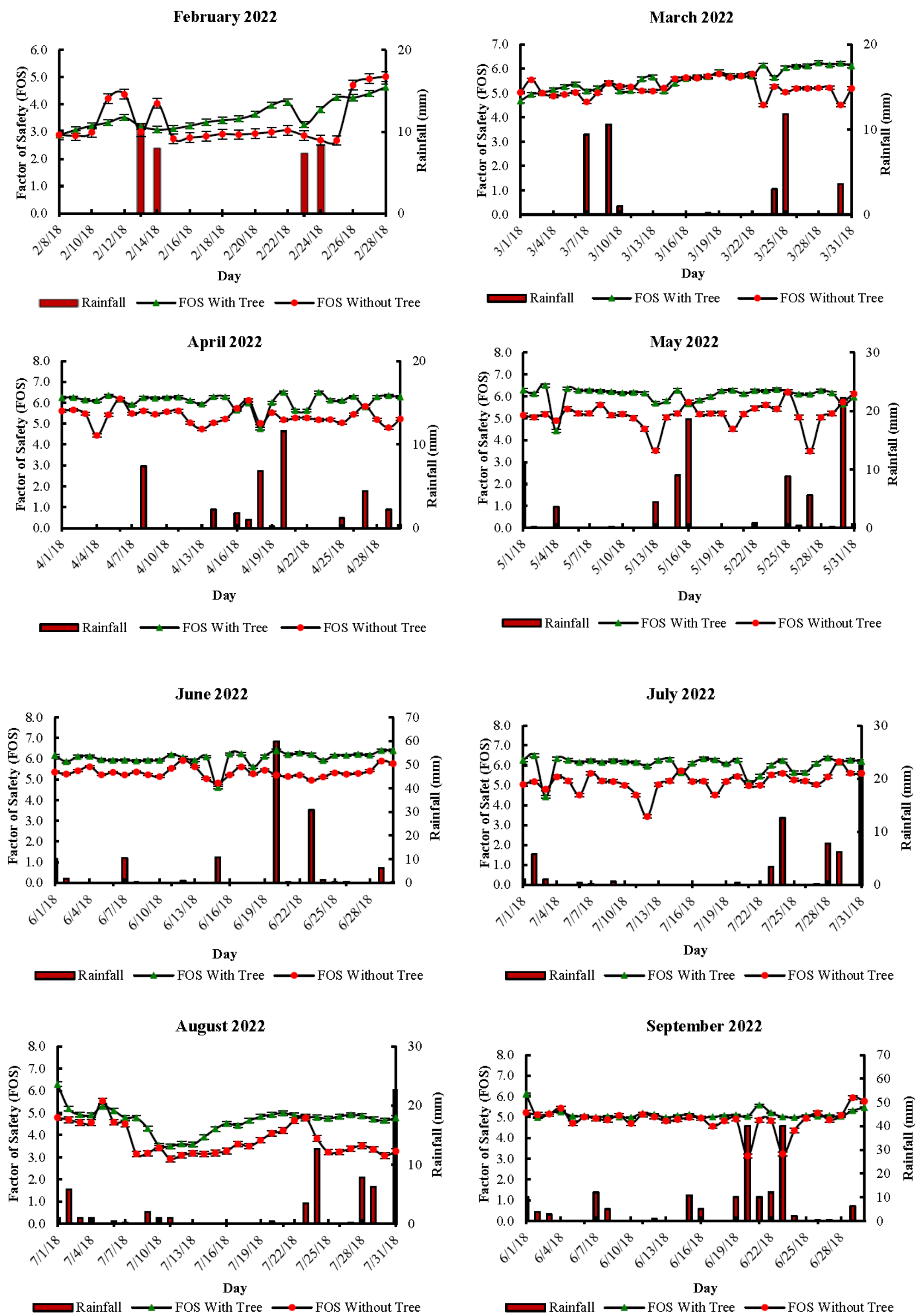


**Figure 17:** Soil matric suction variations with a critical slip surface and slices on tropical residual soil slope with and without the existence of *Alstonia Angustiloba* mature tree.

matric suction on 22nd February 2022 to 25th February 2022 shows insignificant differences due to the overlapping of the error bars. However, the soil matric suction recorded at the slope with the existence of *Alstonia Angustiloba* mature tree is higher collated to the slope without a tree. Based on Figures 9(a) and 9(b), both of the unsaturated slope with or without the existence of *Alstonia Angustiloba* mature tree coherent to the antecedent rainfall event shows insignificant differences in soil matric suction on 16th April 2022 to 20th April 2022 as the error bars do not overlap with each other. However, the soil matric suction value recorded for the slope without the tree is slightly lower than the slope with the existence of the mature tree. The scenario is the same for the soil matric suction with or without the existence of the mature tree during the prolonged antecedent rainfall (see Figures 10(a) and 10(b)) that occurred on 20th June 2022 to 26th June 2022.

Based on the soil matric suction recorded during the prolonged dry condition (13th February 2022, 18th February 2022 and 22nd February 2022) presented in Figures 11 to 13, the data were analyzed based on the various soil matric suction at a different depth, distance and station with the existence of *Alstonia Angustiloba* mature tree and without the existence of the mature tree. On 13th February 2022 (Slope Area), there is a significant difference between the soil matric suction of the slope without a tree at various depths with the soil matric suction at different depths and distances of the slope with the existence of mature trees on the top as the error bars did not overlap with each other. At the flat area (FA), there are no significant differences between the tree water uptake due to the overlapping of the error bars at various depths and distances. On 18th February 2022 (Slope Area), there is significant differences in tree water uptake between the slope with or without a tree at the top at a different distance except at the deepness of 1.5 m and 2.0 m as the data overlapped with the soil suction of 4.4 m distance. At the deepness of 0.25 m to 2.0 m with various distances from the mature tree, the soil matric suction is significant, except at the deepness of 1.5 m to 2.0 m as the tree water uptake of the slope without the tree is overlapped with the tree water uptake of the slope with the existence of the mature tree at the distance of 4.4 m with a deepness of 1.5 m and 2.0 m. At the flat area (FA), the soil matric suction without the existence of a mature tree is significant to the soil matric suction at various depths and a distance of 2.2 m and 1.1 m. However, coherent to the overlapping error bars between the soil matric suction at the deepness of 0.5 m to 2.0 m, the soil matric suction of the slope without the tree is not significant to the slope with the presence of the tree at the distance of 4.4 m.

On 22nd February 2022, at the SA and FA, the tree water uptake at the slope without a tree is significantly different from the tree water uptake of the slope with the existence of the mature tree at the deepness of 0.25 m to 2.0 m for all depth except at the deepness of 1.5 m and 2.0 m (1.1 m and 4.4 m distance from the mature tree). Based on Figure 17, most of the FOS value of the slope without the existence of the *Alstonia Angustiloba* mature tree for eight (8) months of field monitoring shows significant differences with the FOS value of the slope with the existence of the mature tree as most of the data did not overlap with each other except when the rainfall precipitation is high which reduce the FOS of the unsaturated slope.

The one-way ANOVA was conducted to examine the mathematical significant difference between the four (4) independent variables (rainfall precipitation, distance of tensiometer from the tree, depth of slope and station area) observed in this study at various conditions (intense rainfall, antecedent rainfall, prolonged antecedent rainfall and prolonged dry condition). Based on the one-way ANOVA, there is a significant difference between the four (4) independent variables (at $P<0.05$, P-value = $2.25 \times 10^{-70}$). Therefore, to specify which parameters contributed to the difference between the means, the Fisher's Least Significant Difference (LSD) was performed as tabulated in Table 3 coherent with the one-way ANOVA conducted. There are six (6) analyses conducted for the LSD; all of the analyses accepted the $H_0$ (Accept the $H_0$ claim at Average Difference < LSD, where the LSD = 0.4147). The analysis that contributed to the existence of the statistically significant difference is tabulated in Table 3. In reference to Table 3, there is a significant difference between the rainfall intensity with the

**Table 3:** Determination of specific parameters that affect the soil matric suction based on Fisher's Least Significant Difference.

| Mean | Absolute Mean Difference | | Remarks |
|---|---|---|---|
| | **Mean Diff.** | **Value** | |
| $\bar{x}_1$ | $\bar{x}_1$-$\bar{x}_2$ | 5.83 | Difference is significant at p = 0.05, LSD = 0.04147 |
| | $\bar{x}_1$-$\bar{x}_3$ | 7.35 | |
| | $\bar{x}_1$-$\bar{x}_4$ | 7.90 | |
| $\bar{x}_2$ | $\bar{x}_2$-$\bar{x}_3$ | 1.52 | |
| | $\bar{x}_2$-$\bar{x}_4$ | 2.07 | |
| $\bar{x}_3$ | $\bar{x}_3$-$\bar{x}_4$ | 0.55 | |

**Note:** $\bar{x}_1$, Rainfall Precipitation; $\bar{x}_2$, Distance of tensiometers from Tree; $\bar{x}_3$, Depth of Slope; $\bar{x}_4$, Station Area.

**Table 4:** Determination of the relationship between four (4) parameters studied according to Pearson's Correlation Coefficient.

| Parameter | A | B | C | D |
|---|---|---|---|---|
| **A** | 1.0 | $8.63x10^{-16}$ | $6.94x10^{-17}$ | 0 |
| **B** | $8.63x10^{-16}$ | 1.0 | $-5.1x10^{-17}$ | 0 |
| **C** | $6.94x10^{-17}$ | $-5.1x10^{-17}$ | 1.0 | 0 |
| **D** | 0 | 0 | 0 | 1.0 |

**Note:** A, Rainfall Precipitation; B, Distance of Tensiometers from the Tree; C, Depth of Slope; D, Station Ar

distance of tensiometers from the tree, depth of the slope and the slope station at a mean difference of 5.83, 7.35 and 7.90 respectively. Moreover, at a mean difference of 1.52 and 2.07, there are also significant differences between the distance of the tensiometers with the depth of the slope and the station area respectively. The differences between the depth of the slope and the station area are also proved at a mean difference of 0.55. The LSD was suggested by Xue *et al*. (2021) and Ai *et al*. (2021) for the mean separation.

Table 4 shows the Pearson's correlation coefficient performed to determine the correlation between the variables observed in this study. Ai *et al.* (2022) investigated that a correlation value which is below 0.4 is considered as weak correlation, above 0.4 is a strong correlation and no correlation exists with the correlation value reaching zero. Based on the table, there is a very weak correlation exists among the three (3) independent variables (rainfall precipitation, distance of tensiometers from the tree and depth of slope) observed in this study as the correlation value is reaching zero except for the station area showing no correlation exits with the other variables.

## CONCLUSIONS

This investigation examined the effect of an *Alstonia Angustiloba* tree at the top of a slope on the tree water uptake dispersions on tropical residual soil. Results showed that changes in climatic conditions resulted in variations in tree water uptake profiles, especially on a slope with a tree at the top. The normal range of cutting slope arithmetic and the tree location at the top of the slope were considered, and the matric suction profiles at a certain depth and distance from the tree were presented and illustrated. These results showed that a single mature tree can greatly contribute to water extraction from the residual soil. The comparison of the FOS value of a tropical residual soil slope with and without a tree showed that mature trees induced acceleration to increase tree water uptake, leading to a 53.00% increase in the FOS value. Pearson's correlation coefficient showed no correlation between rainfall intensity, distance of tensiometers from the tree, depth of slope and station area. The use of the *Alstonia Angustiloba* mature tree contributed to the improvement of the FOS up to 53.00% from 2.17 to 4.57.


## FUNDING

The study leading to these results received funding from Universiti Malaysia Pahang (UMP) under Grant Agreement Number RDU202701, RDU223309 and from Hokoku Engineering Co. Ltd. under Grant Agreement Number UIC201503.

## ACKNOWLEDGEMENTS

The authors would like to acknowledge the Universiti Malaysia Pahang (UMP) and Hokoko Engineering Co. Ltd for financing this research through the International Grant, Project Number UIC201503, and UMP Matching Grant, Project Number RDU202701, RDU223309. The authors also would like to acknowledge all of the reviewers involved in reviewing this manuscript. The cooperation given by all parties involved in this research is greatly acknowledged.


## AUTHOR CONTRIBUTIONS

All authors contributed to the study conception and design. Material preparation, data collection and analysis were performed by MSIZ, MH and MFZ. The first draft of the manuscript was written by MSIZ and all authors commented on previous versions of the manuscript. All authors read and approved the final manuscript.

## CONFLICT OF INTEREST

The authors declare that they have no known competing financial interests or personal relationships that could have appeared to influence the work reported in this paper.

## REFERENCES


Ai, X., Wang, L., Xu, D., Rong, J., Ai, S., Lie, S., Li, C., & Ai, Y., 2021. Stability of artificial soil aggregates for cut slope restoration: A case study from the subalpine zone of southwest China. Soil Tillage Research, 209, 104934.

Ai, Z., Zhang, J., Liu, H., Liang, C., Xue, S., & Lie, G., 2020. Influence of slope aspect on the macro- and micronutrients in Artemisia sacrorum on the Loess Plateau in China. Environmental Science and Pollution Research, 27, 20160-20172.

Awang, H., Salmanfarsi, A.F., Zaini, M.S.I., Mohamad Yazid, M.A.F., & Ali, M.I., 2021. Investigation of groundwater table under rock slope by using electrical resistivity imaging at Sri

Jaya, Pahang, Malaysia. IOP Conference Series: Earth and Environmental Science, 682, 012017.

Basahel, H., & Mitri, H., 2017. Application of rock mass classification systems to rock slope stability assessment: A case study. Journal of Rock Mechanics and Geotechnical Engineering, 9, 993-1009.

Bastola, S., Cai, M., & Damjanac, B., 2020. Slope stability assessment of an open pit using lattice-spring-based synthetic rock mass (LS-SRM) modeling approach. Journal of Rock Mechanics and Geotechnical Engineering, 12, 927-942.

Biddle, G., 1979. 2-Tree Root Damage to Buildings—An Arboriculturist's Experience. The International Journal of Urban Forestry, 3, 397-412.

Bouzid, D.A., 2022. Finite element analysis of slope stability by expanding the mobilized principal stress Mohr's circles-development, encoding and validation. Journal of Rock Mechanics and Geotechnical Engineering, 14, 1165-1179.

Chen, J., He, B., Wang, X., Ma, Y., & Xi, W., 2013. The effects of Herba Andrographitis hedgerows on soil erodibility and fractal features on sloping cropland in the Three Gorges Reservoir Area. Environmental Science and Pollution Research, 20, 7063-7070.

Feng, S., Liu, H.W., & Ng, C.W.W., 2020. Analytical analysis of the mechanical and hydrological effects of vegetation on shallow slope stability. Computers and Geotechnics, 118, 103335.

Fredlund, D.G., Xing, A., Fredlund, M.D., & Batbour, S.L., 1996. The relationship of the unsaturated soil shear strength to the soil-water characteristic curve. Canadian Geotechnical Journal, 33, 440-448.

Goh, J.R., Ishak, M.F., Zaini, M.S.I., & Zolkepli, M.F., 2020. Stability analysis and improvement evaluation on residual soil slope: Building cracked and slope failure. IOP Conference Series: Materials Science and Engineering, 736, 072017.

Hasan, M., Zaini, M.S.I., Yie, L.S., Masri, K.A., Jaya, R.P., Hyodo, M., & Winter, M.J., 2021a. Effect of optimum utilization of silica fume and eggshell ash to the engineering properties of expansive soil. Journal of Materials Research and Technology, 14, 1401-1418.

Hasan, M., Zaini, M.S.I., Hong, N.A.W., Wahab, A., Masri, K.A., Jaya, R.P., Hyodo., Winter, M.J., Sholichin, M., & Haribowo, R., 2021b. Sustainable ground improvement method using encapsulated polypropylene (PP) column reinforcement. IOP Conference Series: Earth and Environmental Science, 930, 012016.

Hasan, M., Zaini, M.S.I., Zulkafli, A.S., Wahab, A., Masri, K.A., Jaya, R.P., Hyodo., Winter, M.J., Sholichin, M., Haribowo, R., & Zulkafli, M.S., 2021c. Geotechnical properties of bauxite: A case study in Bukit Goh, Kuantan, malaysia. IOP Conference Series: Earth and Environmental Science, 930, 012098.

Hasan, M., Zaini, M.S.I., Hashim, N.A.A., Wahab, A., Masri, K.A., Jaya, R.P., Hyodo, M., Winter, M.J., Sholichin, M., & Haribowo, R., 2021d. Stabilization of kaolin clay soil reinforced with single encapsulated 20 mm diameter bottom ash column. IOP Conference Series: Earth and Environmental Science. 930, 012099.

Hongde, W., Dongli, S., Xiaoqin, S., Shengqiang, T., & Yipeng, Z., 2021. Analysis of unsaturated shear strength and slope stability considering soil desalinization in a reclamation area in China. Catena, 196, 104949.

Huat, B.B.K., Ali, F.H., & Abdullah, A., 2005. Shear strength parameters of unsaturated tropical residual soils of various weathering grades. Electronic Journal of Geotechnical Engineering, 17, 33-46.

Ishak, M.F., & Zaini, M.S.I., 2018. Physical analysis work for slope stability at Shah Alam, Selangor. Journal of Physics: Conference Series, 995, 012064.

Ishak, M.F., B.K.K, Zaini, M.S.I., & Zolkepli, M.F., 2018. Investigation and Monitoring of Groundwater Level: Building Crack Near to IIUM Kuantan. International Journal of Engineering Technology and Sciences, 5, 51-56.

Ishak, M.F., Zolkepli, M.F., Yunus, M.Y.M., Ali, N., Kassim, A., & Zaini, M.S.I., 2021a. The effect of tree water uptake on suction distribution in tropical residual soil slope. Physics and Chemistry of the Earth, Parts A/B/C, 121, 102984.

Ishak, M.F., Zolkepli, M.F., Yunus, M.Y.M., Ali, N., Kassim, A., & Zaini, M.S.I., 2021b. Verification of tree induced suction with numerical model. Physics and Chemistry of the Earth, Parts A/B/C, 121, 102980.

Kardani, N., Zhou, A., Nazem, M., & Shen, S.L., 2021. Improved prediction of slope stability using a hybrid stacking ensemble method based on finite element analysis and field data. Journal of Rock Mechanics and Geotechnical Engineering, 13, 188-201.

Liang, Z., Liu, H., Zhao, Y., Wang, Q., Wu, Z., Deng, L., & Gao, H., 2020. Effects of rainfall intensity, slope angle, and vegetation coverage on the erosion characteristics of Pisha sandstone slopes under simulated rainfall conditions. Environmental Science and Pollution Research, 27, 17458-17467.

Ni, J.J., Leung, A.K., Ng, C.W.W., & Shao, W., 2018. Modelling hydro-mechanical reinforcements of plants to slope stability. Computers and Geotechnics, 95, 99-109.

Nyambayo, V.P., & Potts, D.M., 2010. Numerical simulation of evapotranspiration using a root water uptake model. Computers and Geotechnics, 37, 175-186.

Oberhollenzer, S., Tschuchnigg, F., & Schweiger, H.F., 2018. Finite element analyses of slope stability problems using non-associated plasticity. Journal of Rock Mechanics and Geotechnical Engineering, 10, 1091-1101.

Pradhan, S.P., & Siddique, T., 2020. Stability assessment of landslide-prone road cut rock slopes in Himalayan terrain: A finite element method based approach. Journal of Rock Mechanics and Geotechnical Engineering, 12, 59-73.

Rahardjo, H., Aung, K.K., Leong, E.C., & Rezaur, R.B., 2004. Characteristics of residual soils in Singapore as formed by weathering. Engineering Geology, 73, 157-169.

Rees, S.W., & Ali, N., 2006. Seasonal water uptake near trees: A numerical and experimental study. Geomechanics and Geoengineering, 1, 129-138.

Rees, S.W., & Ali, N., 2012. Tree induced soil suction and slope stability. Geomechanics and Geoengineering, 7, 103-113.

Schiavon, J.A., de Hollanda Cavalcanti Tsuha, C., & Thorel, L., 2019. Monotonic, cyclic and post-cyclic performances of single-helix anchor in residual soil of sandstone. Journal of Rock Mechanics and Geotechnical Engineering, 11, 824-836.

Wang, J., Gu, Y., Wang, H., & Li, Z., 2021. Investigation on the treatment effect of slope wetland on pollutants under different hydraulic retention times. Environmental Science and Pollution Research, 28, 9107-9119.

Woodman, N.D., Smethurst, J.A., Roose, T., Powrie, W., Meijer, G.J., Knappet, J.A., & Dias, T., 2020. Mathematical and computational modelling of vegetated soil incorporating hydraulically-driven finite strain deformation. Computers and Geotechnics, 127, 103754.

Xue, S., Huang, N., Fan, J., Liu, Z., Ye, Y., He, Y., Hartley, W., & Zhu

F., 2021. Evaluation of aggregate formation, stability and pore characteristics of bauxite residue following polymer materials addition. Science of the Total Environment, 765, 142750.

Yue, L.J., Ishak, M.F., Zaini, M.S.I., & Zolkepli, M.F., 2019. Rainfall induced residual soil slope instability: buidling cracked and slope failure. IOP Conference Series: Materials Science and Engineering, 669, 012004.

Zaini, M.S.I., Ishak, M.F., & Zolkepli, M.F., 2019. Forensic assessment on landfills leachate through electrical resistivity imaging at Simpang Renggam in Johor, Malaysia. In: IOP Conference Series: Materials Science and Engineering, 669, 012005.

Zaini, M.S.I., Ishak, M.F., & Zolkepli, M.F., 2020a. Monitoring soil slope of tropical residual soil by using tree water uptake method. IOP Conference Series: Materials Science and Engineering, 736, 072018.

Zaini, M.S.I., Ishak, M.F., Zolkepli, M., Wahap, M.S., Sidek, J.I.J., Yasin, A.M., Zolkepli, M.N., Mohmad Sidik, M.H., Mohd Arof, K.Z., & Abu Talib, Z., 2020b. Granite exploration by using Electrical Resistivity Imaging (ERI): A case study in Johor. International Journal of Integrated Engineering, 12, 328-347.

Zaini, M.S.I., Hasan, M., Yie, L.S., Masri, K.A., Jaya, R.P., Hyodo, M., & Winter, M.J., 2022a. The effect of utilizing silica fume and eggshell ash on the geotechnical properties of soft kaolin clay. Jurnal Teknologi, 84, 159-170.

Zaini, M.S.I., Hasan, M., & Zolkepli, M.F., 2022b. Urban landfills investigation for leachate assessment using electrical resistivity imaging in Johor, Malaysia. Environmental Challenges, 6, 100415.

Zaini, M.S.I., Hasan, M., & Jusoh, W.N.B.W., 2023. Utilization of bottom ash waste as a granular column to enhance the lateral load capacity of soft kaolin clay soil. Environmental Science and Pollution Research.

Zaini, M.S.I., & Hasan, M., 2023. Effect of optimum utilization of silica fume and lime on the stabilization of problematic soils. International Journal of Integrated Engineering, 15, 352-366.

Zhang, W., Li, H., Han, L., Chen, L., & Wang, L., 2022. Slope stability prediction using ensemble learning techniques: A case study in Yunyang County, Chongqing, China. Journal of Rock Mechanics and Geotechnical Engineering, 14, 1089-1099.

Zhu, H., & Zhang, L., 2019. Root-soil-water hydrological interaction and its impact on slope stability. Georisk, 13, 349-359.

Zhu, H., & Zhang, L.M., 2015. Evaluating suction profile in a vegetated slope considering uncertainty in transpiration. Computers and Geotechnics, 63, 112-120.

Zhu, H., Zhang, L.M., & Garg, A., 2018. Investigating plant transpiration-induced soil suction affected by root morphology and root depth. Computers and Geotechnics, 103, 26-31.

Zolkepli, M.F., Ishak, M.F., Yunus, M.Y.M., Zaini, M.S.I., Wahap, M.S., Yasin, A.M., Sidik, M.H., & Hezmi, M.A., 2021a. Application of unmanned aerial vehicle (UAV) for slope mapping at Pahang Matriculation College, Malaysia. Physics and Chemistry of the Earth, Parts A/B/C, 123, 103003.

Zolkepli, M.F., Mohamad Rozar, N., Ishak, M.F., Sidik, M.H., Ibrahim, N.A.S., & Zaini, M.S.I., 2021b. Slope mapping using unmanned aerial vehicle (UAV). Turkish Journal of Computer and Mathematics Education, 12, 1781-1789.

Zolkepli, M.F., Ishak, M.F., & Zaini, M.S.I., 2018. Analysis of slope stability on tropical residual soil. International Journal of Civil Engineering Technology, 9, 402-416.

Zolkepli, M.F., Ishak, M.F., & Zaini, M.S.I., 2019. Slope stability analysis using modified Fellenius's and Bishop's method: IOP Conference Series: Materials Science and Engineering, 527, 012004.

*Manuscript received 5 November 2022;*
*Received in revised form 22 April 2023;*
*Accepted 3 May 2023*
*Available online 26 May 2023*